Proc. Natl. Acad. Sci. USA
Vol. 77, No. 2, pp. 804–807, February 1980
Biochemistry

Enhancement of phospholipid transfer from Sendai virus to erythrocytes is mediated by target cell membrane

(phospholipid exchange/envelope fusion/cell fusion/spin label)

KAZUMICHI KURODA, TOYOZO MAEDA, AND SHUN-ICHI OHNISHI

Department of Biophysics, Faculty of Science, Kyoto University, Kyoto 606, Japan

Communicated by Harden M. McConnell, November 5, 1979

ABSTRACT **Transfer of phospholipid from the envelope of Sendai virus to erythrocyte membrane was measured by using spin-labeled phosphatidylcholine. The transfer was enhanced autocatalytically above a threshold dose (about five adsorbed viruses per cell). There was an inflection point in the time course of transfer, after which the transfer was greatly accelerated. The time to reach the inflection point became shorter with increased viral dose. The transfer reaction was markedly enhanced above 19°C and the inflection point was observed above this temperature. There was negligible transfer from trypsin-treated virus to erythrocyte membrane, but the transfer was greatly enhanced by intact virus. The enhancement was larger with increased amount of intact virus, and the inflection point was observed in the transfer curves. All the kinetic data can be satisfactorily analyzed by a model which assumes that the virus modifies the cell membrane at the attachment site, the modification is propagated in the membrane, and transfer of phospholipid to the modified sites is greatly enhanced. The propagation rate is estimated as $\approx 10^{-11}$ cm^2 s^{-1} and the activation energy as 13 kcal mol^{-1} (54 kJ mol^{-1}). The viral F glycoproteins are suggested as a possible entity for the modification and its propagation: they are introduced into the target cell membrane by envelope fusion, diffuse laterally, and enhance both phospholipid exchange and envelope fusion with viruses attached to the membrane sites.**

Membrane fusion constitutes a critical step in many cellular processes such as phagocytosis, secretion, and incorporation of integral proteins into cell membrane (1). Cell fusion induced by Sendai virus (2), a synonym for hemagglutinating virus of Japan (HVJ), provides a suitable model system for studying dynamic membrane phenomena, and many studies have sought to elucidate the mechanism (3). The overall reaction involves several key steps: adsorption of virus to cell membrane, aggregation of cells, envelope fusion with cell membrane, hemolysis, and fusion of cells. We have been studying the fusion mechanism by measuring intermembrane phospholipid transfer, using spin-labeled HVJ or spin-labeled erythrocytes (RBCs) (4, 5). The membranes were labeled with spin-labeled phosphatidylcholine (PtdCho*) to an extent of 10–15% of total phospholipid so that the transfer of PtdCho* to unlabeled membranes could be easily followed *in situ* by the peak height increase of the electron spin resonance (ESR) spectrum. It has been found that the transfer from HVJ envelopes to RBC membrane is governed by the viral F glycoprotein and constitutes an initial key step in the membrane fusion. The transfer is markedly dependent on the incubation temperature and is greatly accelerated above 19°C. HVJ activates transfer from otherwise inactive influenza virus or trypsin-treated HVJ (HVJ_{trp}) to RBC membrane.

The present study is focused on the effect of increasing dosages of HVJ on the transfer from HVJ to RBC and on the HVJ-activated transfer from HVJ_{trp} to RBC. The temperature dependence of the transfer reaction is also studied in more detail. The results strongly suggest a membrane-mediated enhancement of the effect of HVJ on the cells.

The publication costs of this article were defrayed in part by page charge payment. This article must therefore by hereby marked "*advertisement*" in accordance with 18 U. S. C. §1734 solely to indicate this fact.

MATERIALS AND METHODS

Virus. HVJ, Z strain, was used throughout. Preparation, purification, trypsinization, and radioiodination of the virus were carried out as described (4, 5). Almost all F protein was split off by the trypsin treatment, and the virus lost its phospholipid transfer activity, as well as hemolysis and fusion activities. Radioiodinated virus was used to determine the fraction of the adsorbed virus. The virus concentration was determined as hemagglutinating units (HAU) or by protein concentration. When necessary, the number of adsorbed virus particles was calculated, assuming 1 HAU = 2.4×10^7 virions (6). Virus was spin-labeled with PtdCho* as described (4, 5). Briefly, virus (25,000–51,200 HAU) was suspended in 1 ml of sonicated PtdCho* vesicles (1 mg/ml) and incubated at 37°C for 5–6 hr. After washing with Tris-buffered saline (140 mM NaCl/5.4 mM KCl/20 mM Tris·HCl, pH 7.6) containing bovine serum albumin and then with the buffer only, the spin-labeled virus (HVJ*) was suspended in the buffer and centrifuged lightly to remove aggregates.

RBCs and Ghosts. Human RBCs were obtained from a blood bank and used within 2 weeks after the blood had been drawn. The cells were washed three times in Tris-buffered saline. Ghosts were prepared by hypotonic hemolysis in 5 mM sodium phosphate buffer, pH 8, and incubated at 37°C for 60 min in Tris-buffered saline for resealing.

Assay of Transfer of PtdCho*. Transfer of PtdCho* from the viral envelope to RBC membrane was measured by the peak height increase in the ESR spectrum as described (4, 5). Briefly, 0.3 ml of 10% (vol/vol) RBC was mixed at 0°C with 0.9 ml of HVJ* or HVJ^*_{trp} and HVJ at various concentrations, kept for 15 min, and centrifuged at $450 \times g$ for 3 min. The agglutinated cell pellet was taken into a quartz capillary tube and the ESR spectrum was measured periodically at 37°C or at various temperatures with a JEOLCO Model ME-X spectrometer. The central peak height relative to the height at time 0 was plotted against incubation time.

RESULTS

Dependence of Phospholipid Transfer on Viral Dose. The phospholipid transfer reaction was markedly dependent on the number of virus particles adsorbed on the cell surface. Fig. 1 shows the increase in the ESR peak height when various amounts of HVJ* were added to a fixed number of RBCs and incubated at 37°C. The peak height increase was small and was almost linear below a threshold viral dose (Fig. 1, curve a).

Abbreviations: HVJ, hemagglutinating virus of Japan; PtdCho*, spin-labeled phosphatidylcholine (12-nitroxide stearate at the 2 position); HVJ*, HVJ containing PtdCho* in the envelope; HVJ_{trp}, trypsin-treated HVJ; HAU, hemagglutinating units; RBC, erythrocyte; ESR, electron spin resonance.

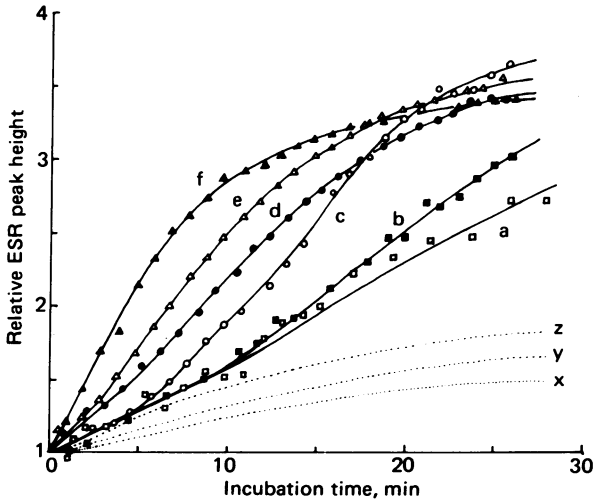

FIG. 1. Transfer of PtdCho* from HVJ to RBC membrane as a function of the viral dose. To 0.3 ml of 10% (vol/vol) RBC, 0.9 ml of various concentrations of HVJ* was added at 0°C, and the ESR spectrum of the cell aggregates was measured at 37°C periodically. The central peak height relative to the initial height was plotted against time. HVJ* (final concentration): a, 120; b, 260; c, 500; d, 1270; e, 2700; and f, 5400 HAU/ml. The dotted curves represent transfer of PtdCho* from HVJ to RBC ghost membrane under equivalent conditions. HVJ* (final concentration): x, 348; y, 696; and z, 2782 HAU/ml.

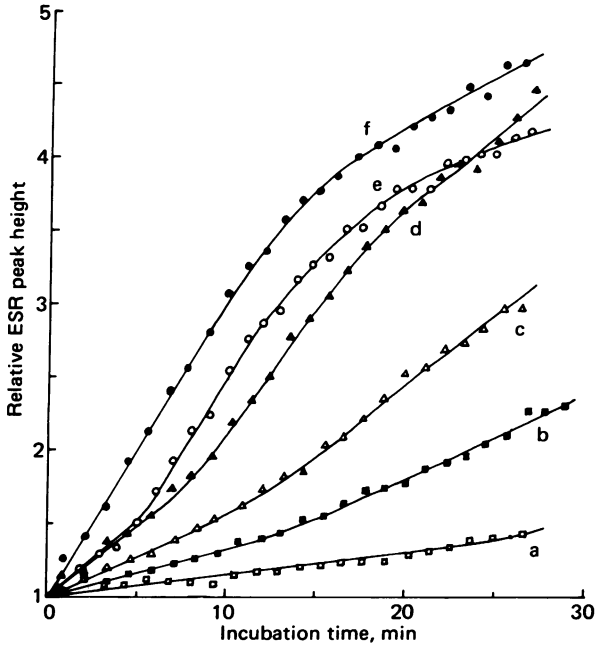

FIG. 2. Activated transfer of PtdCho* from HVJ_{trp} to RBC membrane by HVJ. To 0.3 ml of 10% (vol/vol) RBC, 0.9 ml of HVJ^*_{trp} (final 260 HAU/ml) and various concentrations of HVJ were added and the ESR spectrum was measured at 37°C periodically. HVJ (final concentration): a, 0; b, 40; c, 160; d, 320; e, 640; and f, 1280 HAU/ml.

When the dose increased above the threshold, the peak height increase became larger and markedly curved (Fig. 1, curves b–e). Moreover, an inflection point after which the transfer rate was increased appeared in the curves. The characteristic time to reach the inflection point, t_c, became shorter with an increase of virus dose. The number of adsorbed virus particles per cell at the threshold was approximately 5.

In striking contrast to intact RBCs, the transfer to RBC ghosts remained slow over a wide range of viral doses (378 to 18,548 HAU/ml) and only slightly dependent on dose (dotted curves in Fig. 1). A considerable fraction of the transfer (about 50% of the curve x) was independent of viral F glycoproteins.

Dependence of HVJ-Activated Transfer on Dose. The transfer from HVJ_{trp} to RBC membrane is activated by HVJ (5). This activated transfer was also markedly dependent on the dose of HVJ. Fig. 2 shows time course of ESR peak height increase when a fixed amount of HVJ^*_{trp} and various amounts of HVJ were adsorbed to RBCs and incubated at 37°C. Curve a, a control without added HVJ, shows the background low level of transfer from HVJ_{trp} lacking viral F protein. Curves b–f show marked enhancement by HVJ. The enhancement became larger with an increase of HVJ dose and an inflection point was observed in the curves. The characteristic time t_c became shorter with increasing amounts of HVJ.

When the target cells were replaced by RBC ghosts, only slight activation by HVJ was observed. The ESR peak height increase remained small when HVJ^*_{trp} and a large dose of HVJ (12,800 HAU/ml) were adsorbed to ghosts and incubated at 37°C. The transfer curve is situated lower than curve a in Fig. 2.

Enhancement of Transfer Mediated by Target Cell Membrane. The autocatalytic nature of transfer from HVJ and the characteristic activation of transfer from HVJ_{trp} strongly suggest the presence of an enhancement mechanism of the effects of HVJ mediated by the target cell membrane: the virus causes modification in the cell membrane, the modification is propagated in the membrane, and transfer of phospholipid to the modified membrane sites is enhanced (Fig. 3). According to this model, the inflection point will appear when the number of virus activated in unit time becomes maximal. The characteristic time t_c should be determined by the most probable distance r_m between the adsorbed viruses (Fig. 3*B*).

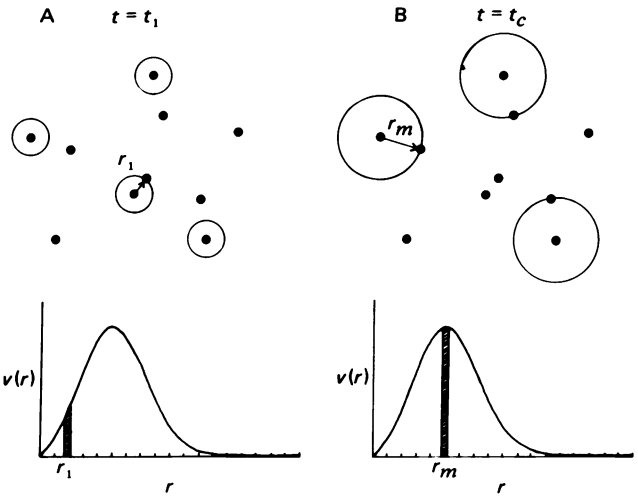

FIG. 3. Enhancement of transfer of phospholipids by modification of the target cell membrane and its propagation. (*A*) Virus (•) modifies the cell membrane at the attached site and the modification propagates in the membrane to r_1 in time t_1. The transfer from the virus bound to the modified membrane site is enhanced. The number of viruses activated in the time interval t_1 and $t_1 + \Delta t$ is indicated by the shaded area in $v(r)$ (one in the upper drawing). Δt is related to Δr by $\Delta t = (t/D)^{1/2} \Delta r$. (*B*) In time t_c, the modification travels to a distance of r_m at which the number of viruses activated in unit time Δ. is maximal (three in the upper drawing). The distribution of virus on the cell surface was assumed to be random. The number of virus located between r and $r + dr$ from a virus is given by $v(r) = A(r/w) \exp[-(r - r_a)^2/2w^2]$, in which w is the width parameter for the distribution.

A relationship between t_c and r_m may be derived by simple considerations. Suppose the modification propagates in the cell membrane with a diffusion constant D and the average squared distance of propagation $\bar{R}^2$ in time t is given by

$$\bar{R}^2 = 4Dt. \quad [1]$$

The characteristic time is then

$$t_c = r_m^2/4D. \quad [2]$$

Multiplying Eq. 2 by π leads to an approximate relationship

$$t_c = (S/4\pi D)(1/V), \quad [3]$$

in which S is the surface area of cell and V the number of adsorbed virus per cell. The characteristic time should be inversely proportional to V and the slope should be related to the propagation constant D. The experimental t_c was obtained from Figs. 1 and 2 and similar data and is plotted against V^{-1} in Fig. 4*A*. The result shows a linear relationship in agreement with the model. The data points for the autocatalytic and the activated transfer reactions were on the same line. The propagation constant D was estimated from the slope as 1.6×10^{-11} cm^2 s^{-1}, taking $S = 200\ \mu m^2$.

Transfer by Phospholipid Exchange and Envelope Fusion. The phospholipid transfer from viral envelope to RBC membrane occurs at least partly through exchange of phospholipids between the two membranes (5). The number of PtdCho* molecules, n, transferred to the cell membrane by this mechanism is given by

$$n = N_0V_0[1 - \exp(-kt)], \quad [4]$$

in which k is the rate constant of the exchange, N_0 the initial number of PtdCho* molecules per virus, and V_0 the initial number of adsorbed virus per cell. Phospholipid exchange also exists before the enhancement, although it is much slower.

Viral phospholipids may also be transferred to the cell membrane by envelope fusion followed by rapid lateral diffusion. It is probable that transfer by this mechanism is also included in the observed transfer because hemolysis occurs under the experimental conditions of the transfer measurements. Virus-induced hemolysis has been correlated with envelope fusion (7, 8). The kinetic equation for transfer by envelope fusion is formally the same as that for transfer by phospholipid exchange. We only need to replace k in Eq. 4 by the probability of envelope fusion per unit time.

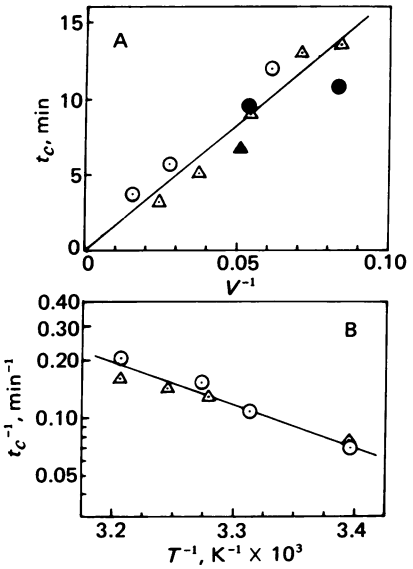

FIG. 4. Dependence of the characteristic time t_c on the number of adsorbed virus V and on the incubation temperature T. (*A*) ⊙ and ▲ represent data for HVJ*–RBC and HVJ*$_{trp}$–HVJ–RBC systems, respectively. Filled and open points are data in different series of experiments. (*B*) HVJ*–RBC system (cf. Fig. 5). ⊙ and ▲ represent data in different series of experiments.

The time course of ESR peak height increases can be simulated by calculations based on the above model. The calculation is lengthy but straightforward and is done with the aid of a microcomputer (to be published elsewhere). Agreement between the simulated and observed transfer curves is satisfactory. It is sufficient to say here that the curves have inflection points near t_c given by Eq. 2.

Temperature Dependence of the Transfer Reaction. The transfer reaction is strongly dependent on the incubation temperature (4). Fig. 5 shows the dependence when HVJ*–

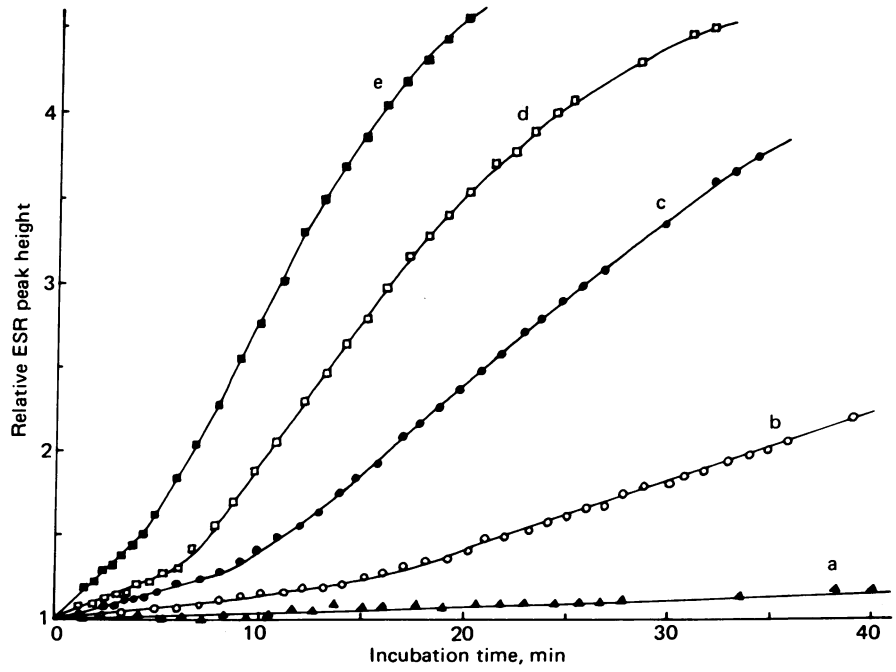

FIG. 5. Temperature dependence of transfer reaction from HVJ to RBC membrane. HVJ* (final 1000 HAU/ml) and RBC were mixed at 0°C and ESR spectra of the cell aggregates were measured at various temperatures: a, 19°C; b, 23°C; c, 29°C; d, 32°C; and e, 37°C.

RBC aggregates are incubated at various temperatures. The transfer was negligibly small below 19°C (curve a) but markedly accelerated at higher temperatures (curves b–e). The inflection point was observed in the accelerated curves. t_c became shorter with increasing temperature.

The temperature dependence fits well the scheme of the membrane-mediated enhancement mechanism of transfer. The decrease of t_c with increasing temperature is primarily due to an increase in the propagation rate of modification in the cell membrane. The temperature dependence of t_c is derived from Eq. **2** as

$$t_c^{-1} = K \exp(-\Delta E/RT), \quad [5]$$

in which D in Eq. **1** is assumed to have the form of $\exp(-\Delta E/RT)$, ΔE is the activation energy for the propagation, R is the gas constant, and K is a proportionality constant. Experimental t_cs were obtained from Fig. 5 and t_c^{-1} is plotted on a logarithmic scale against T^{-1} in Fig. 4*B*. The data points are on a straight line, supporting the model. The activation energy estimated from the slope is 13 kcal mol^{-1} (54 kJ mol^{-1}).

Increases in the rate of phospholipid exchange and of envelope fusion, in addition to the increased propagation rate, should also contribute to the enhancement of transfer above 19°C. Freezing of transfer below 19°C may be attributed to some structural change in the target cell membrane.

DISCUSSION

The present study has shown a catalytic enhancement of the effect of Sendai virus on RBCs by modification of the target cell membrane. Analysis of kinetic data on phospholipid transfer indicates that the modification propagates in the cell membrane rather slowly with a diffusion constant of the order of 10^{-11} cm^2 s^{-1} and with activation energy of 13 kcal mol^{-1}. No enhancement occurs, therefore, within the time scale of observation when the number of adsorbed virus particles on the cell surface is small (<5). In the absence of enhancement, the transfer is slow and increases almost linearly with time. With enhancement, the transfer reaction becomes explosively rapid after a certain threshold time that is dependent on the viral dose and incubation temperature. This autocatalytic amplification should be essential to the biological action of cell fusion by HVJ. In fact, virus at lower doses, corresponding approximately to the threshold amount, does not cause appreciable fusion of RBCs. Negligible fusion of RBC ghosts by HVJ is in line with the lack of significant enhancement of transfer. Recently, conditions for fusion of ghosts have been investigated (9–12); ghosts loaded with bovine serum albumin were found to be more easily fused (11). However, an order of magnitude larger dose of virus and longer incubation were required. The transfer from HVJ* to the albumin-loaded ghosts was slow and not much dependent on the viral dose (unpublished observation). The insensitivity of ghosts to fusion by HVJ can therefore be explained by the small amplification of the effect of virus.

What is the mechanism of the enhancement? What is involved in the modification and its propagation in the target cell membrane? We assume that the viral glycoproteins F and HANA are implanted into the cell membrane by envelope fusion, diffuse laterally, and, when they come to the membrane sites where other virus particles are bound, the F glycoproteins enhance phospholipid exchange as well as envelope fusion with the bound virus. In the beginning—i.e., before enhancement—there is a certain probability of phospholipid exchange and envelope fusion between the virus and the target cell membrane. These events are also governed by the F glycoproteins. The protein has a hydrophobic amino terminus (13), which may strongly interact and perturb the adjacent membrane. The membrane perturbation should be the common cause for the two processes. Once envelope fusion has occurred, the implanted F protein may be able to move to sites of attachment of other virus particles, perturb the viral membranes, and enhance phospholipid exchange and envelope fusion. The observed slow propagation constant for the modification and high activation energy are compatible with the model because restricted lateral mobility of RBC integral proteins has been reported with a diffusion constant of 4×10^{-11} cm^2 s^{-1} at 37°C (14). We are now directly measuring lateral diffusion of implanted viral glycoproteins in fused RBC membranes by fluorescence photobleaching recovery. Preliminary data give values of the order of 10^{-11} cm^2 s^{-1} at room temperature for the diffusion constant.

Several lines of evidence have shown that HVJ causes aggregation of RBC integral proteins (11, 15) and the intracellular spectrin–actin meshworks are involved in aggregate formation (11). Protein aggregation is accompanied by formation of protein-free lipid bilayer area. Because the membrane fluidity of intact RBCs is low, probably due to interaction with proteins, the formation of a protein-free lipid area would increase fluidity as observed by PtdCho* in the membrane (5). Implanted viral proteins may be able to move laterally in the lipid area.

The enormous difference between RBCs and ghosts in the reaction with HVJ may be related to modification of the spectrin–actin meshworks on hemolysis. This modification may impair the capability of the meshworks to form aggregates of integral proteins. This has been actually observed in ghosts that have reacted with HVJ under normal conditions (11). Lateral diffusion of implanted viral proteins may be hampered in these circumstances. Another factor for the enormous difference may be that the probability of envelope fusion with ghosts is smaller than that with intact RBCs.

1. Poste, G. & Nicolson, G. L., eds. (1978) *Cell Surface Reviews*, Membrane Fusion (North-Holland, Amsterdam), Vol. 5.
2. Okada, Y. (1958) *Biken J.* **1**, 103–110.
3. Poste, G. & Nicolson, G. L., eds. (1977) *Cell Surface Reviews*, Virus Infection and the Cell Surface (North-Holland, Amsterdam), Vol. 2.
4. Maeda, T., Asano, A., Ohki, K., Okada, Y. & Ohnishi, S. (1975) *Biochemistry* **14**, 3736–3741.
5. Maeda, T., Asano, A., Okada, Y. & Ohnishi, S. (1971) *J. Virol.* **21**, 232–241.
6. Okada, Y., Nishida, S. & Tadokoro, J. (1961) *Biken J.* **4**, 209–213.
7. Homma, M., Shimizu, K., Shimizu, Y. K. & Ishida, N. (1976) *Virology* **71**, 41–47.
8. Shimizu, Y. K., Shimizu, K., Ishida, N. & Homma, M. (1976) *Virology* **71**, 48–60.
9. Peretz, H., Toister, Z., Laster, Y. & Loyter, A. (1974) *J. Cell Biol.* **63**, 1–11.
10. Lalazar, A., Michaeli, D. & Loyter, A. (1977) *Exp. Cell Res.* **107**, 79–88.
11. Sekiguchi, K. & Asano, A. (1978) *Proc. Natl. Acad. Sci. USA* **75**, 1740–1744.
12. Lalazar, A. & Loyter, A. (1979) *Proc. Natl. Acad. Sci. USA* **76**, 318–322.
13. Gething, M. J., White, J. M. & Waterfield, M. D. (1978) *Proc. Natl. Acad. Sci. USA* **75**, 2737–2740.
14. Fowler, V. & Branton, D. (1977) *Nature (London)* **268**, 23–26.
15. Bächi, T., Aguet, M. & Howe, C. (1973) *J. Virol.* **11**, 1004–1012.